

Quasi-single helicity spectra in the Madison Symmetric Torus

L. Marrelli

Consorzio RFX, Associazione EURATOM-ENEA per la fusione, Corso Stati Uniti, 4-35127 Padova, Italy

P. Martin and G. Spizzo

Consorzio RFX, Associazione EURATOM-ENEA per la fusione, Corso Stati Uniti, 4-35127 Padova, Italy and Istituto Nazionale di Fisica della Materia, UdR Padova, Italy

P. Franz

Consorzio RFX, Associazione EURATOM-ENEA per la fusione, Corso Stati Uniti, 4-35127 Padova, Italy

B. E. Chapman, D. Craig, J. S. Sarff, T. M. Biewer, S. C. Prager, and J. C. Reardon

Department of Physics, University of Wisconsin, 1150 University Avenue, Madison, Wisconsin 53706

(Received 23 January 2002; accepted 9 April 2002)

Evidence of a self-organized collapse towards a narrow spectrum of magnetic instabilities in the Madison Symmetric Torus [R. N. Dexter, D. W. Kerst, T. W. Lovell, S. C. Prager, and J. C. Sprott, *Fusion Technol.* **19**, 131 (1991)] reversed field pinch device is presented. In this collapsed state, dubbed quasi-single helicity (QSH), the spectrum of magnetic modes condenses spontaneously to one dominant mode more completely than ever before observed. The amplitudes of all but the largest of the $m=1$ modes decrease in QSH states. New results about thermal features of QSH spectra and the identification of global control parameters for their onset are also discussed. © 2002 American Institute of Physics. [DOI: 10.1063/1.1482766]

The self-organization of toroidal plasmas into preferred magnetic equilibria constitutes an interesting feature relevant to many natural and laboratory plasmas. The self-organizing dynamics typically involve complicated nonlinear interactions among many magnetic instabilities. The reversed field pinch (RFP)^{1,2} is an example of a plasma configuration in which such a collection of spatial Fourier modes has a large effect on the macroscopic behavior of the plasma. In the RFP these modes underlie the magnetic field generation mechanism called “dynamo,” and can cause the magnetic field lines to wander chaotically, leading to rapid energy loss. This is what typically happens in the standard multiple helicity (MH) regime, where many instabilities with poloidal mode number $m=1$ but different toroidal number and similar amplitudes are simultaneously present in the plasma, driving a turbulent dynamo. An approach to reduce the magnetic chaos, which has been suggested by theoretical work,^{3–5} is to create a self-organized state which is dominated by a single $m=1$ mode, leading to well formed, nonchaotic helical magnetic surfaces. This is called the single helicity (SH) state, in which a laminar instead of a turbulent dynamo acts, and the symmetry breaking required to have a stationary RFP equilibrium in a resistive plasma is provided by the nonlinear saturation of a resistive kink mode.⁵ The SH state is not the helical Taylor state.⁵ Experimental RFP plasmas in which the spectrum of $m=1$ modes condenses spontaneously to one dominant mode with a well defined toroidal number n have been observed in several devices.^{6–9} In the RFX device these spectra have been observed to last for the entire discharge, and a helical coherent structure, hotter than the plasma nearby, is detected in the plasma core.¹⁰ The ratio of the dominant to the other secondary modes is much smaller than

for the theoretical SH state, hence these experimental spectra are referred to as quasi-single helicity (QSH).

In this Letter we report new results from the Madison Symmetric Torus (MST) RFP, in which the spectrum of magnetic modes condenses spontaneously to one dominant mode more completely than ever before observed.^{6–10} Moreover, for the first time it is observed that the spectra are characterized not only by the increase of one $m=1$ mode, but also by the simultaneous decrease of the other $m=1$ modes. We will also discuss new results on the identification of control parameters for the onset of the QSH spectra. Evidence of a hot core helical structure will also be illustrated.

MST¹¹ (minor radius $a=0.52$ m, major radius $R_0=1.5$ m, plasma current up to 0.5 MA) has at least two important features for QSH dynamics: it is the lowest aspect ratio RFP device in operation ($A=R_0/a\approx 3$), and it is characterized by a very smooth and close shell. At small A , fewer $m=1$ modes of significant amplitude are expected to be present in the plasma.¹² The smooth magnetic boundary might reduce field errors acting as seeds of magnetic stochasticity. Various experimental conditions have been explored in MST, including different global plasma parameters, plasma current waveforms and the application of pulsed poloidal current drive (PPCD),^{13–15} a technique consisting of the induction of a poloidal electric field at the plasma edge to suppress magnetic fluctuations. The discharges studied for this Letter have plasma current I_p , line averaged electron density n_e and reversal parameter $F (=B_\phi(a)/\langle B_\phi \rangle)$ respectively, in the ranges $0.2 < I_p < 0.4$ MA, $0.5 < n_e < 2 \times 10^{19} \text{ m}^{-3}$, $-1.0 < F < 0$. F and Θ [where $\Theta = B_\theta(a)/\langle B_\phi \rangle$] are two parameters traditionally used to describe RFP magnetic equilibria.² $B_\theta(a)$ and $B_\phi(a)$ are the poloidal and toroidal magnetic field at the wall, whereas

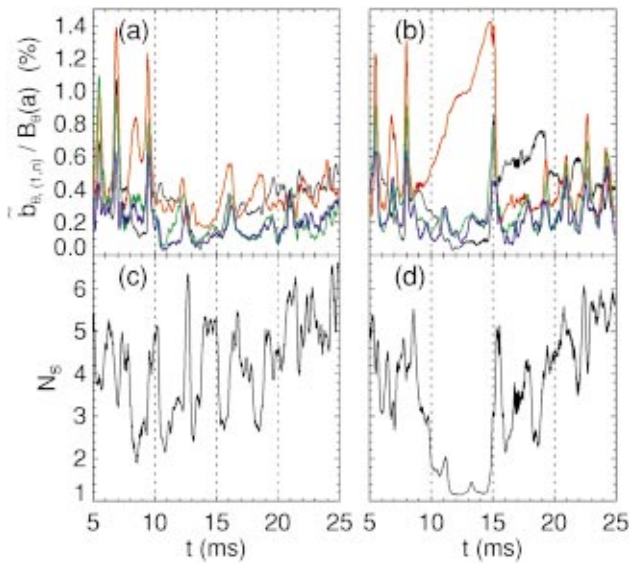


FIG. 1. (Color) Time evolution of the magnetic $m = 1$ modes measured with a toroidal array of magnetic field sensing coils at the plasma surface. Amplitudes of $m = 1$, $n = 5 - 8$ and the spectral spread N_s for a MH plasma (a), (c) and for a spontaneous QSH plasma (b), (d) are shown (black: $n = 5$; red: $n = 6$; green: $n = 7$; blue: $n = 8$).

$\langle B_\phi \rangle$ is the cross-section averaged toroidal magnetic field. Magnetic evidence of QSH spectra are observed in MST: Fig. 1 compares the $m = 1$ magnetic mode behavior for two 0.4 MA plasmas: one with a MH and one with a QSH spectrum. Figure 1(a) shows the time evolution of the $m = 1$ modes amplitudes (instantaneous spatial Fourier decomposition based on a toroidal array of 32 poloidal field pick-up coils¹⁶) for the MH plasma. Since MHD instabilities eigenfunctions are global, edge magnetic fluctuations measurements are representative of the core behavior.² All the $m = 1$ modes have roughly the same amplitude. This is not the case for the spontaneous QSH plasma shown in Fig. 1(b). In this case the QSH spectrum is evident between 10 and 15 ms, where the ($m = 1$, $n = 6$) mode dominates the toroidal spectrum with an amplitude normalized to the edge poloidal field $b_{\theta,(1,6)} / B_\theta(a) < 1.4\%$. Simultaneously a reduction of the secondary $m = 1$ modes is also observed, a feature rather typical in MST, as we shall show also in Fig. 3. To characterize quantitatively the shape of magnetic spectra, the time evolution of the spectral spread number, N_s , is plotted in Figs. 1(c), 1(d). N_s is defined as $N_s = [\sum_n (b_{\theta,(1,n)}^2 / \sum_{n=5}^{14} b_{\theta,(1,n)}^2)^2]^{-1}$.¹² While in the MH case N_s

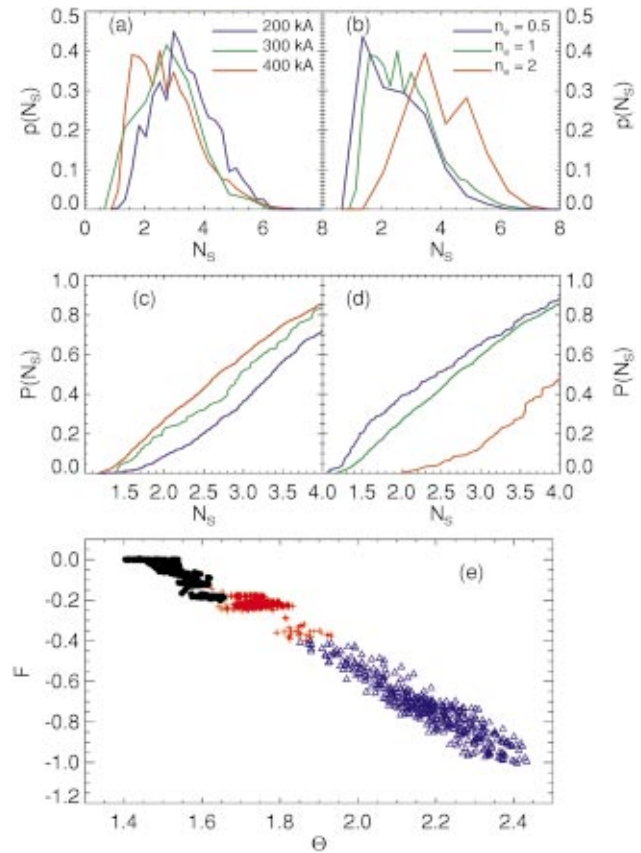


FIG. 2. (Color) Probability density distribution function of N_s values (a) for three different values of plasma current $I_p \approx 200, 300$ and 400 kA at $n_e \approx 1 \times 10^{19} \text{ m}^{-3}$ and $F \approx -0.2$, and (b) for three different values of plasma density $n_e \approx 0.5, 1, 2 \times 10^{19} \text{ m}^{-3}$ at $I_p \approx 400$ kA. Integrals $P(N_s) = \int_1^{N_s} p(N'_s) dN'_s$: (c) for the $p(N_s)$ functions of frame (a); (d) for the $p(N_s)$ functions of frame (b). (e) Location of the QSH plasmas in the $F - \Theta$ plane. Black dots corresponds to QSH spectra with dominant $n = 5$, red crosses to $n = 6$ and blue triangles to QSH during PPCD with dominant $n = 6$.

never decreases below 2 [Fig. 1(c)], in the QSH period [Fig. 1(d)] N_s approaches the value of 1, which is the value for a pure Single Helicity state.

The large MST dataset of reproducible discharge enables a statistical analysis of the main features of QSH states, and the search for experimental control parameters which favor their onset. The analysis has been carried out in a set of ≈ 770 discharges, where the plasma quantities have been sampled over contiguous 0.2 ms time intervals, for a total of about 56,000 points. Since many MST discharges are af-

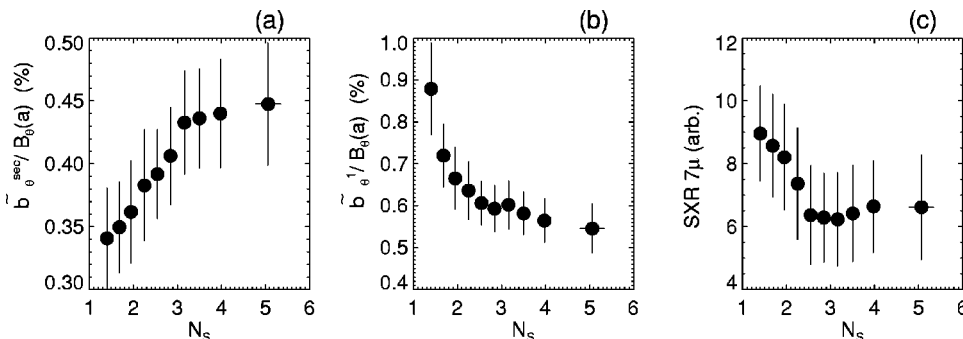


FIG. 3. (a) Normalized rms secondary modes, b_θ^{sec} vs N_s . (b) Normalized rms of all $m = 1$ modes, $\sqrt{\sum b_\theta^2} / B_\theta(a)$, vs N_s . (c) SXR emission measured through a $7 \mu\text{m}$ thick beryllium filter vs N_s .

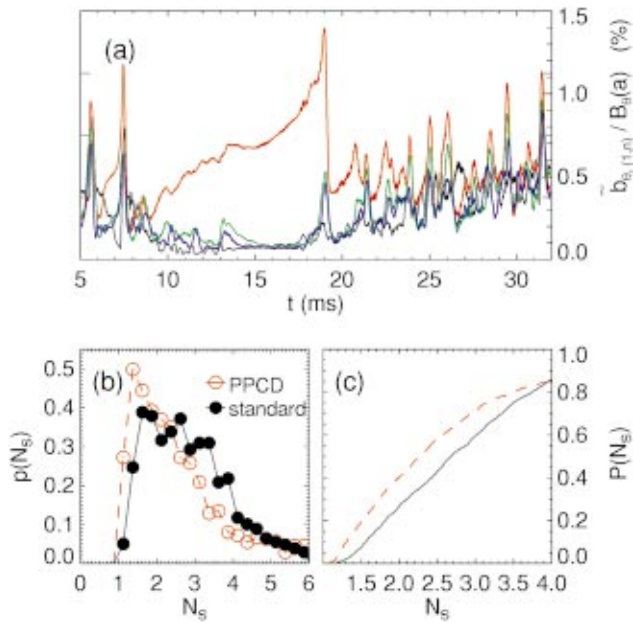


FIG. 4. (Color) (a) Time evolution of the magnetic $m=1$ mode amplitudes during a PPCD shot where a QSH spectrum appears. (b) Probability density distributions of N_s for plasmas with and without PPCD. (c) Probability curve of obtaining a given value of N_s for PPCD and standard plasmas.

fects by discrete, quasi-periodic relaxation events called sawtooth crashes,¹⁷ the sampling is performed in periods free from crashes. Plasma current is a parameter that plays a role in the probability of getting a QSH spectrum. In Fig. 2(a) the probability density distribution function $p(N_s)$ of N_s values is plotted for three sets of discharges, whose flat-top current was pre-programmed to $I_p \approx 206 \pm 3$, 313 ± 4 and 425 ± 5 kA. The sets include 2,800 points from 290 different discharges with $F \sim -0.18 \pm 0.01$, $n_e \sim 1 \pm 0.1 \times 10^{19} \text{ m}^{-3}$. $p(N_s)$ is normalized such that $\int p(N_s) dN_s = 1$. The $p(N_s)$ curve is displaced towards lower values for the higher current. This indicates a higher probability to obtain QSH spectra with higher plasma current. Medium-low values of the electron density also make more likely the achievement of

QSH spectra. In Fig. 2(b) $p(N_s)$ is plotted for three sets of discharges, whose flat-top plasma density was pre-programmed to $n_e = 0.5 \pm 0.1, 1 \pm 0.1, 2 \pm 0.2 \times 10^{19} \text{ m}^{-3}$. The sets include 2000 points from 169 different discharges. All these discharges have $I_p = 410 \pm 10$ kA and $F = -0.19 \pm 0.01$. The plasmas with $n_e \approx 2 \times 10^{19} \text{ m}^{-3}$ have, on average, broader $m=1$ spectra. Figures 2(c) and 2(d) summarize the current and density dependence by showing the integral $P(N_s) = \int_1^{N_s} p(N'_s) dN'_s$ of the distributions of Figs. 2(a) and 2(b) vs N_s . The $P(N_s)$ curves corresponding to higher current and lower density are above the others. In QSH regimes the $m=1$ magnetic mode spectrum peaks around toroidal mode numbers $n_0=5$ or 6, and very rarely around $n_0=7$. These modes are resonant near the magnetic axis according to typical MST safety factor profiles, i.e., those with n closest to $1/q(0) \approx 2R/a$. The toroidal mode number of the dominant mode can be selected by varying the magnetic equilibrium, and in particular the F and Θ parameters. Figure 2(e) shows the location in the $F-\Theta$ plane of QSH plasmas. They are separated according to toroidal mode number of the dominant instability. Plasmas with dominant mode $n=5$ are characterized by weak or zero reversal (i.e., $F \geq -0.2$) and by $\Theta \leq 1.65$. A QSH spectrum with a dominant $n=6$ corresponds to $\Theta \geq 1.65$, which corresponds to a lower on-axis safety factor.

The statistical analysis shows that spontaneous QSH states are characterized by a reduction of the secondary $m=1$ mode amplitudes. This result is described in Fig. 3. In particular, Fig. 3(a) shows the behavior of the normalized rms of the secondary modes, $b_{\theta}^{\text{sec}} = \sqrt{\sum_{\text{sec}} b_{\theta,(1,m)}^2} / B_{\theta}(a)$, vs N_s . Each point represents an average over many data with N_s in a narrow range. The normalized rms of the secondary modes increases with N_s , i.e., it is lower in QSH conditions. This is not the case for the rms of all $m=1$ modes [Fig. 3(b)], which also includes the dominant mode and is higher in the QSH spectra. QSH plasmas are therefore characterized by an overall larger $m=1$ modes energy than MH plasmas, but the energy is concentrated in one mode in QSH compared to many in MH.

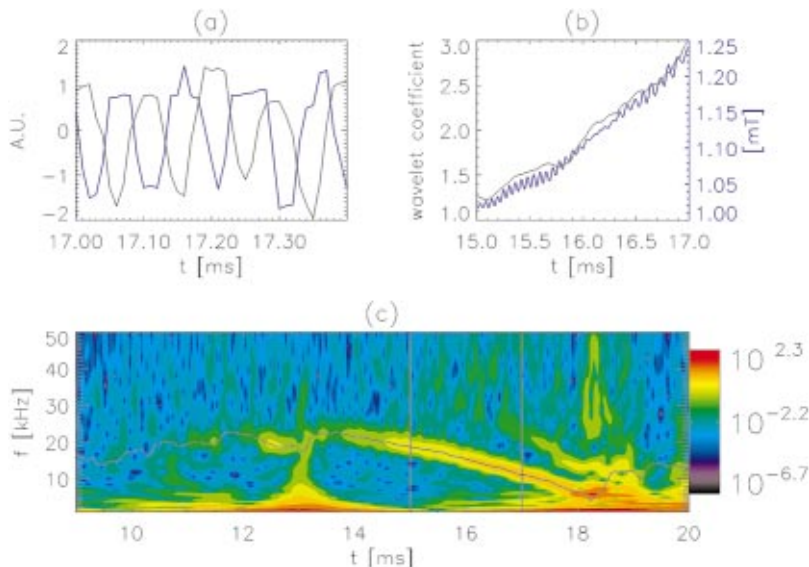


FIG. 5. (Color) (a) Oscillations in two SXR channels during a QSH state. (b) Time evolution of the SXR oscillation envelope and of the dominant mode amplitude. (c) Wavelet spectrum of one SXR signal. The black curve superimposed to the spectrum gives the time evolution of the dominant magnetic mode rotation frequency.

The difference between MH and QSH spectra in MST is not only limited to magnetic properties. In Fig. 3(c) the soft-x-ray (SXR) emission measured through a $7\ \mu\text{m}$ thick beryllium filter is plotted vs N_s . This SXR emission is a function of the electron density, temperature, and of impurity concentration. All the discharges used for this figure have similar density. The highest values of the SXR emission occur with QSH spectra, a result that is consistent with a hotter plasma core.

The probability of obtaining long-lasting QSH spectra at 0.4 MA is enhanced by the application of PPCD, as shown by the analysis of optimized PPCD¹⁵ experiments at $I_p \approx 0.4$ MA. The time evolution of the $m=1$ mode amplitudes for a typical 0.4 MA QSH during PPCD is reported in Fig. 4(a). Figure 4(b) shows the comparison of probability density distribution function of N_s values, $p(N_s)$, for plasmas without PPCD (136 discharges for a total of 1668 points) and with PPCD (108 discharges for a total of 1400 points). The PPCD distribution is shifted towards lower values of N_s : the integral of the two distributions of Fig. 4(b), shown in Fig. 4(c), indicates that the probability of getting a N_s value less than 2 [$P(2) = \int_1^2 p(N_s) dN_s$] with PPCD is almost double that without PPCD. In PPCD experiments performed at 0.2 MA this trend is not observed. It is interesting that the presence of a QSH spectrum during PPCD, with the increase of the amplitude of one mode, does not alter the energy confinement. This can be explained as follows: the total magnetic fluctuation energy can increase during PPCD with QSH, provided that the energy is concentrated in one mode. The large reduction of the secondary modes contributes to the decrease of magnetic stochasticity. The increase of the dominant instability does not counteract this process (as one could expect from a classical island overlapping criterion¹⁸) but could generate in the core a hot coherent magnetic structure with closed helical magnetic flux surfaces, similar to that observed in RFX.¹⁰ As shown in Fig. 2(c), the QSH spectra obtained during PPCD experiments have dominant $n=6$, following the same trend obtained with spontaneous QSH plasmas.

SXR measurements are consistent with the presence of a hotter $m=1$ helical structure in the plasma core, produced by the dominant MHD mode and associated with the formation of closed helical flux surfaces. During QSH phases the signals from two SXR detectors display out-of-phase oscillations superimposed on the slow trend: an example is shown in Fig. 5(a), for a QSH spectrum obtained during PPCD. Since the two detectors view the plasma core along two lines of sight crossing the equatorial plane on opposite sides with

respect to the magnetic axis and the magnetic modes rotate, this is a signature of an $m=1$ oscillation. The wavelet spectrum of these signals shows that these oscillations have a well defined frequency which coincides with the poloidal rotation frequency of the dominant $m=1$ mode [Fig. 5(c)]. In addition, we note that the amplitude of the SXR oscillation varies with time, and is proportional to the amplitude of the dominant $m=1$ magnetic mode [Fig. 5(b)].

Although the theoretical SH state without magnetic chaos has not yet been experimentally achieved, the observed collapse to a narrow spectrum suggests that a broad spectrum of magnetic fluctuations is not an unavoidable feature of the RFP. It remains to be determined whether there are other experimental control parameters which can extend these observed QSH spectra to the pure, stationary SH state.

ACKNOWLEDGMENTS

Four of the authors (P. F., L. M., P. M., G. S.) thank the whole MST team for the hospitality during their visits, and the RFX team for the fruitful discussions.

- ¹S. C. Prager, *Plasma Phys. Controlled Fusion* **41**, A129 (1999).
- ²S. Ortolani and D. D. Schnack, *Magnetohydrodynamics of Plasma Relaxation* (World Scientific, Singapore, 1993).
- ³S. Cappello and R. Paccagnella, *Phys. Fluids B* **4**, 611 (1992).
- ⁴J. M. Finn, R. A. Nebel, and C. C. Bathke, *Phys. Fluids B* **4**, 1262 (1992).
- ⁵D. F. Escande, S. Cappello, F. D'Angelo, P. Martin, S. Ortolani, and R. Paccagnella, *Plasma Phys. Controlled Fusion* **42**, B243 (2000).
- ⁶Y. Hirano, Y. Maejima, T. Shimada, Y. Yagi, S. Sekine, I. Hirota, H. Sakakita, T. J. Baig, G. Serianni, and H. Ji, *Proceedings of Contributed Papers*, 16th IAEA Fusion Energy Conference, Montreal, 1996 (IAEA, Vienna, 1997), Vol. 2, p. 95.
- ⁷P. Nordlund and S. Mazur, *Phys. Plasmas* **1**, 4032 (1994).
- ⁸B. E. Chapman, Ph.D. thesis, University of Wisconsin, Madison, 1997.
- ⁹P. Martin, *Plasma Phys. Controlled Fusion* **41**, A247 (1999).
- ¹⁰D. F. Escande, P. Martin, S. Ortolani *et al.*, *Phys. Rev. Lett.* **85**, 1662 (2000).
- ¹¹R. N. Dexter, D. W. Kerst, T. W. Lovell, S. C. Prager, and J. C. Sprott, *Fusion Technol.* **19**, 131 (1991).
- ¹²Y. L. Ho, D. D. Schnack, P. Nordlund, S. Mazur, H.-E. Satherblom, J. Scheffel, and J. R. Drake, *Phys. Plasmas* **2**, 3407 (1995).
- ¹³J. S. Sarff, N. E. Lanier, S. C. Prager, and M. R. Stoneking, *Phys. Rev. Lett.* **78**, 62 (1997).
- ¹⁴R. Bartiromo, P. Martin, S. Martini, T. Bolzonella, A. Canton, P. Innocente, L. Marrelli, A. Murari, and R. Pasqualotto, *Phys. Rev. Lett.* **82**, 1462 (1999).
- ¹⁵B. E. Chapman, J. K. Anderson, T. M. Biewer *et al.*, *Phys. Rev. Lett.* **87**, 205001 (2001).
- ¹⁶A. F. Almagri, S. Assadi, J. Becksted *et al.*, *Proceedings of Contributed Papers*, Workshop of Physics of Alternative Magnetic Confinement Schemes, Varenna, Italy, 1990, edited by S. Ortolani and E. Sidoni (Societa Italiana di Fisica, Bologna, 1991), p. 223.
- ¹⁷S. Hokin, A. Almagri, S. Assadi *et al.*, *Phys. Fluids B* **3**, 2241 (1991).
- ¹⁸B. Chirikov, *Phys. Rep.* **52**, 265 (1979).